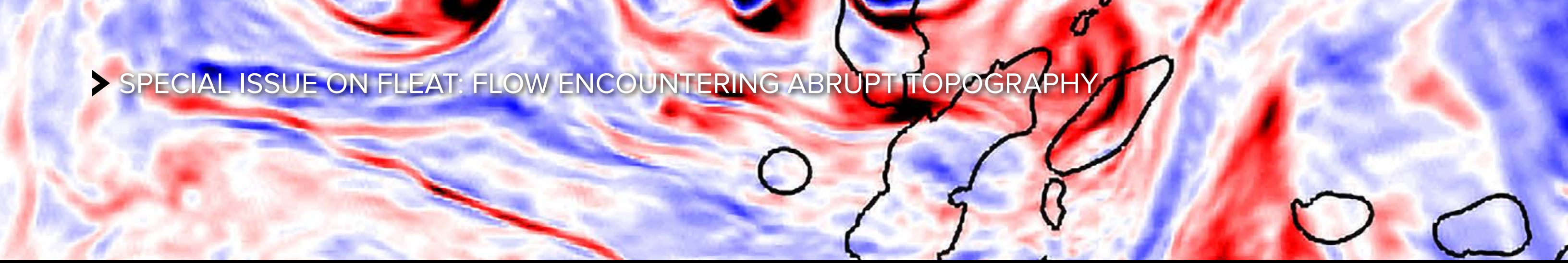

DYNAMICAL DOWNSCALING OF EQUATORIAL FLOW RESPONSE TO PALAU

By Harper L. Simmons, Brian S. Powell, Sophia T. Merrifield, Sarah E. Zedler, and Patrick L. Colin

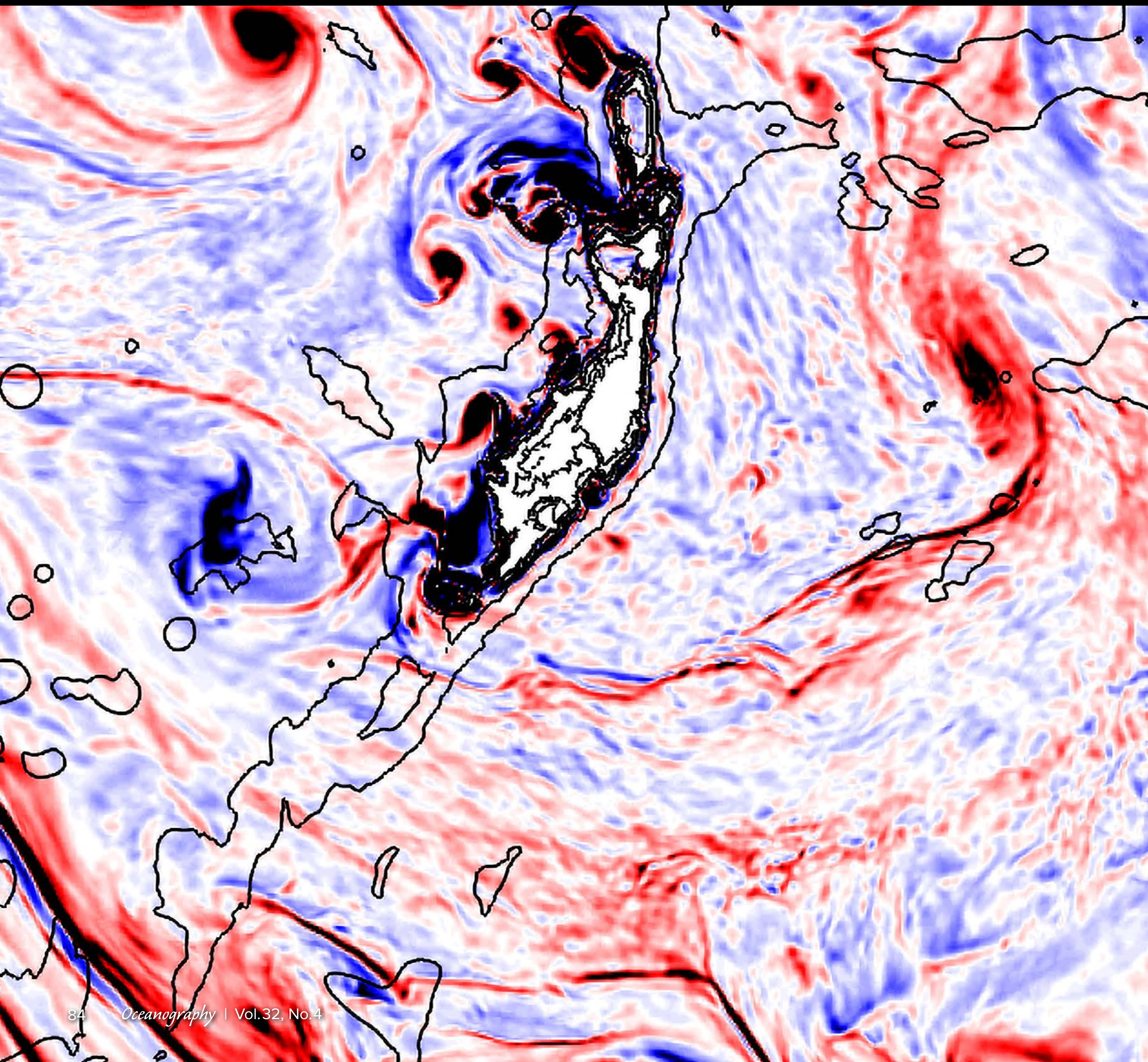

> "These results show that to capture the characteristics of the wake behind the island of Palau (and other similar obstructions to large mean flows) requires model resolution that is many times higher than the typical first baroclinic mode Rossby radius."

ABSTRACT. The wake created by the interaction of equatorial currents with the Palau islands generates small-scale vortices. We aim to identify the significant scales of this vortex wake by studying its structure and variability. We utilize a subkilometer resolution numerical model integrated from May 2016 through April 2017 that is nested within a 2.5 km state estimate hindcast model. The near-Palau flow is highly variable and has very different wake generation characteristics depending on whether the flow is westward or eastward. During westward flow, numerous strong vortices are generated at the northern tip of Velasco Reef and advected hundreds of kilometers to the northwest. During less frequent and less persistent eastward flow, transport develops through the Euchelel Ngeruangl and Kekerel Euchel channels that separate Velasco Reef from the main Palau island group. As this flow encounters the atoll of Kayangel in the channel, it splits and emerges to the east as vortices. During our 2016–2017 study period, these Kayangel eddies were ejected from the channel and advected southward along the eastern coast of Palau while being sheared laterally, and thus the wake did not have a large eastward extent. We find that wake eddies were not well resolved in the 2.5 km state estimate and that more numerous and intense eddies were simulated at higher resolution. Accurate simulations of the wake around such ocean obstructions therefore require subkilometer resolving models.

IN PLAIN WORDS. The turbulent wakes created by the collision of equatorial currents with Palau topography are highly variable in space and time. Intense ocean vortices are generated and can be swept hundreds of kilometers downstream. Simulation of these dynamics requires ocean models that are considerably higher resolution than those in standard use.

INTRODUCTION

The currents of the equatorial western Pacific encounter numerous submarine ridges and island arcs. The interaction of the flow with topography causes a cascade of motions from planetary to small scales. We denote these small scales as submesoscale, meaning that they are unresolved in large-scale, eddy-permitting ocean models, and in our context are of the order of or smaller than the island/reef scales of kilometers to tens of kilometers. These topographic interactions are associated with enhanced upwelling and vertical mixing, processes that have long been known to enhance biological productivity around islands in the form of the so-called "island-mass effect" (e.g., Hamner and Hauri, 1981; Hernandez-Léon, 1991; Dower et al., 1992). Vorticity and energy transfer to small scales are in turn believed to remove energy from the large-scale mean flow of the equatorial current systems. The cascade ultimately feeds energy to the fine and microstructure scales, where instability mechanisms lead to turbulence and dissipation.

The cool, geostrophic westward return flow of the North Pacific Subtropical Gyre referred to as the North Equatorial Current (NEC) is, on average, found between 7°N and 20°N. As the NEC encounters the eastern flank of the Philippines, it bifurcates into the southward-flowing Mindanao Current and the northward-flowing origin of the Kuroshio. The Mindanao Current collides with the northward New Guinea Coastal Current, resulting in the eastward-flowing North Equatorial Countercurrent (NECC), which is highly meandering in the western Pacific, but tends to remain between 3°N and 7°N. These two large-scale flows commonly encounter the islands of Palau, generating significant wakes, and there is interest in understanding how well they can be both represented and predicted in a numerical modeling framework. For predictions and process studies of flows in such regions, it is common to use a high-resolution (on the order of kilometers) model that may be rather numerically expensive. At these latitudes, the submesoscale exists from hundreds of meters to tens of kilometers and would not be fully permitted by a typical regional model.

A great deal of literature is devoted to observational, numerical, and laboratory process studies of flow past headlands and seamounts. Previous numerical studies show that submesoscale topographic wakes are only accurately simulated at high resolutions because the horizontal and vertical scales of separation between bottom boundary layers are small (Gula et al., 2015a,b; Molemaker et al., 2015). Perfect et al. (2018) report on a study of stratified flow past an idealized seamount that focuses on nondimensional characterization of the flow. Selected other studies are those by Heywood et al. (1996), Caldeira et al. (2005), Chang et al. (2013), and further references can be found therein.

In this paper, we examine the flow and vorticity of the wake that is produced as the planetary flows encounter the islands of Palau. This study was conducted as part of the Office of Naval Research's Flow Encountering Abrupt Topography (FLEAT) Departmental Research Initiative.

MODELS

Two distinct model setups were used in this study, one nested within the other. Both use the Regional Ocean Modeling System (ROMS), a free-surface, hydrostatic, primitive equation model discretized with a terrain-following vertical coordinate system (Shchepetkin and McWilliams, 2005). ROMS has been widely used for applications around the globe, from large-scale basin to meter-scale estuarine and brackish water simulations.

The parent model setup will be referred to as the REGION model, configured with a horizontal resolution of 2.5 km. The REGION model uses 25 vertical s-level terrain-following layers with a higher distribution of layers in the upper 250 m. ROMS is a hydrostatic model, which can affect the generation of internal waves; however, as shown in Bergh and Berntsen (2008), the nonhydrostatic component is negligible for the resolution and the significant horizontal flux of energy considered here. The REGION model was in turn nested within an 8 km four-dimensional variational (4D-Var) state-estimate model of the western tropical Pacific, described by Zedler et al. (2019, in this issue), with the tides prescribed spectrally as detailed in Janeković and Powell (2012) to preserve the energy fluxes produced by remote sources. The surface forcing was provided by the state estimate that adjusted the Global Forecasting System (GFS) to better represent the oceanic processes. For this work, we assimilated nearly 6 million observations using the Physical-space Statistical Analysis System 4D-Var (Courtier, 1997) method to produce a new, high-resolution state estimate. These state estimates were performed in three-day windows between February 1, 2016, and April 20, 2017.

The REGION model combined observations from satellites, Argo profiling floats, the Tropical Atmosphere Ocean (TAO) moored buoy array, and the data collected as part of the FLEAT project described in this issue. We used along-track sea surface height anomalies drawn from a variety of satellites and provided by AVISO (https://www.aviso.altimetry.fr) and sea surface temperature data from the Naval Oceanographic Office (NAVO) blended product (May et al., 1998). Additionally, observations of temperature or salinity from Argo and measurements of velocity, temperature, or salinity from TAO were used.

From the FLEAT program, we utilized temperature and salinity observations from 11 Spray glider missions and from SeaSOAR surveys along with radial velocity observations from a high-frequency (HF) radar installation (Merrifield et al., 2019, in this issue). We employed velocity, temperature, and salinity as available from moorings M1, M2, M3, M4, M5, F1, and F3. The output of this 14-month state estimate forms the REGION experiment that was used to force the finer-scale PALAU model presented here.

Our high-resolution PALAU model at 800 m horizontal resolution using 50 s-levels is nested within this 2.5 km state estimate. The REGION state estimate provided lateral boundary conditions with a restoring timescale of 1 day^{-1} for temperature, salinity, free surface elevation, and two- and three-dimensional momentum. Sea surface salinity was restored with a timescale of 1/90 days^{-1}. Surface fluxes were taken from the state estimate adjusted fluxes of the REGION model. Lateral boundary conditions follow the one-way procedure of Mason et al. (2010). As with the state estimate, the nested model boundary conditions were de-tided and then reintroduced spectrally. Both the REGION and PALAU models use the Large et al. (1994) K-profile parameterization (KPP) vertical turbulence closure model. Horizontal diffusion of tracers in the REGION and PALAU models were 60 m^2 s^{-1} and 13 m^2 s^{-1}, and mixing of momentums were 50 m^2 s^{-1} and 9 m^2 s^{-1}, respectively. Quadratic bottom drag in both models was 3×10^{-3}.

BATHYMETRY

A new 100 m resolution bathymetric data set (**Figure 1**) was prepared using multibeam surveys collected by R/V *Roger Revelle* merged with reef survey data prepared by the Coral Reef Research Foundation (CRRF). The CRRF bathymetric data were used to refine the reef/deep ocean boundary for Palau and nearby islands from a variety of sources, including single point surveys, existing reliable hydrographic charts, and satellite and aerial images that reveal the bottom to approximately 60 m depth. For the purpose of preparing model grids, the bathymetric data were gridded to a uniform resolution of 100 m and blended with V19.1 of the global 30-arc-second

Smith and Sandwell (1997) topography, after upsampling to the common 100 m grid resolution. From there, model grid data were prepared by bin-averaging the 100 m to the 2,500 m resolution REGION model grid resolution and to the 800 m grid resolution of the PALAU model. For the PALAU model, the land-water mask was set to 25 m, and special care was used to maintain open channels.

RESULTS

The nested PALAU model was integrated as a series of 12 independent one-month runs covering May 2016 to April 2017. Each monthly run was reinitialized using initial conditions from the REGION run starting with the nearest prior re-initialization of the state estimate (i.e., the August 2016 PALAU integration was initialized July 30, 2016, and run for one month). Our purpose in running in monthly intervals is to examine the evolution of the resolved vs. unresolved flow over 30-day periods. We reinitialize every 30 days to bring the solutions back to consistency with the REGION model. The spinup timescale for the initial cascade of resolved vorticity variance to scales less than 10 km is approximately 12 hours.

A useful parameter for describing the flow is relative vorticity, $\zeta = \partial v/\partial x - \partial u/\partial y$. Here, we scale ζ by Earth's rotational frequency f to form a Rossby number $\mathrm{Ro} = \zeta/f$. The modeled flow past Palau is highly variable in space and time. Westward flow past the northern tip of Velasco Reef exhibits complicated vertical and horizontal structure (Figures 2 and 3), with horizontal shears exceeding $10f$ and vertical shears exceeding 1 m s^{-1} km^{-1}. We find $|\mathrm{Ro}| > 10$ throughout the PALAU domain (i.e., many island lengths away from Palau) and that these large Rossby numbers mainly originate where currents interact with topography. When such large values are found far from Palau, they are a result of advection and straining of the high Ro fluid by the larger-scale (and lower Ro) equatorial currents.

Notable features of the flow in the immediate vicinity of Palau that are evident in a subkilometer simulation are the episodic wakes extending from the north of Velasco during westward flow (Figure 4a), the passages between Velasco and main island group during eastward flow (Figure 4b), and the wake generation at Angaur to the south of the main island group (Figures 1 and 4b). Many of the intense cyclones and anticyclones have $|\mathrm{Ro}| > 10$, and some are as strong as 30, significantly more intense than the peak Ro in the parent REGION model, which reaches 5–10. In addition to the island-induced vortex generation, there are large sheared bands of positive and negative vorticity (e.g., Figure 4a, southwest corner of Palau region). We

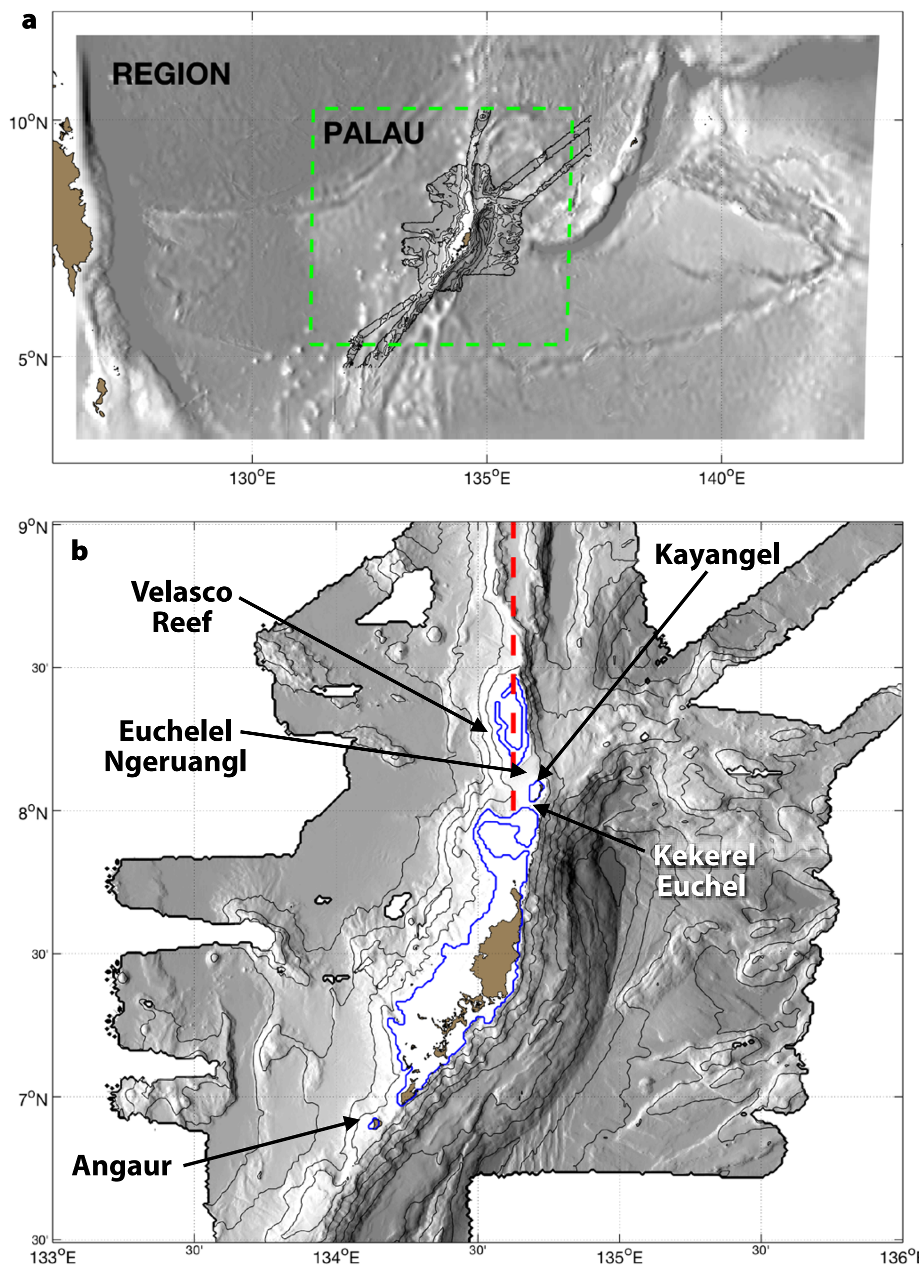

FIGURE 1. (a) The REGION domain extends from 126°15'E, 3°15'N to 143°22'E, 11°47'N, and the PALAU model domain (dashed lines) extends from 131°15'E, 5°15'N to 136°50'E, 10°15'N. (b) Extent of high-resolution bathymetry from ship multibeam and other sources for the PALAU region, subsampled for use in both models. The blue contour near Palau is the 25 m isobath, which defines the PALAU model land-sea mask. Key geographic features referred to in the text are identified. The red dashed line indicates a section running north through Velasco Reef.

examine some of these features both at the surface and at depth during differing flow regimes (Figures 2–4), and summarize some key statistics describing this flow (Figures 5 and 6) to help identify the scales at which the wake exists.

Flow Regimes

As documented by Merrifield et al. (2019, in this issue), surface flow to the east of Velasco and Kayangel is predominantly to the northwest (Figure 3b); however, the flow direction is highly variable. We considered mean flow in the upper 200 m along a north-south section shown in Figure 1 (red dashed line). Along the Velasco line, currents (averaged over three days over the upper 200 m and from 8°30'N to 9°00'N) predominantly come from the southwest and southeast directions (Figure 3a,b). In the oceanographic convention, the dominant flow is therefore to the northwest, similar to the results of Merrifield et al. (2019, in this issue). The effects of the island and ridge on the surface vorticity and near-surface currents can be seen in Figure 4.

During periods of westward flow, a "street" of vortices can be traced back to vorticity production at the tip of Velasco Reef. These vortices are advected to the northwest with the larger-scale flow (Figure 4a). Conversely, during eastward flow such as occurred in August 2016, strong transport through Kekerel Euchel and Euchelel Ngeruangl channels (Figure 4b) creates a wake that emanates from the channels rather than at the tip of Velasco. As the flow encounters Kayangel, it bifurcates and forms a dipole that is advected (or perhaps in part self-propagates) away from Palau. In the

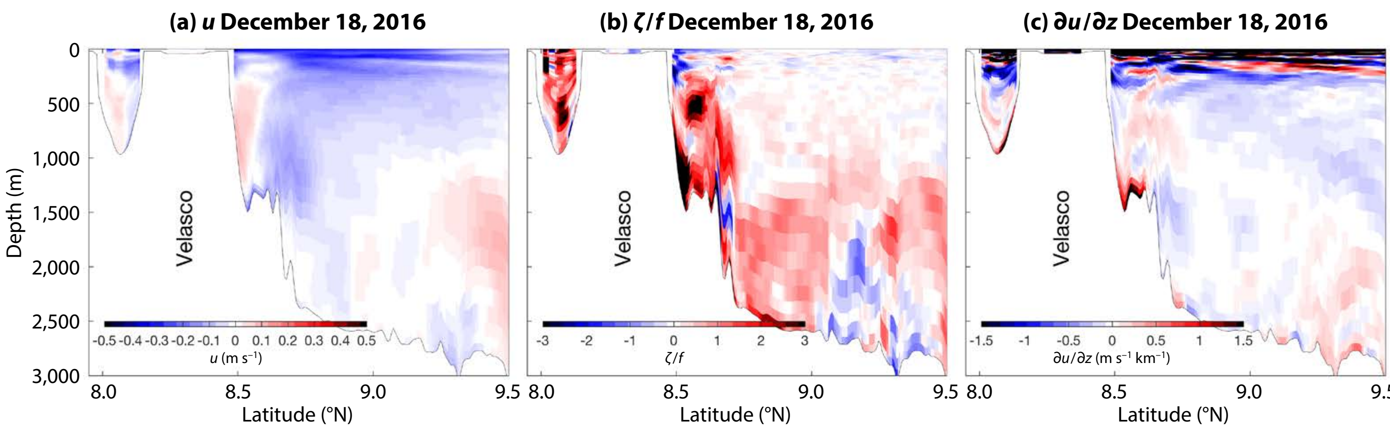

FIGURE 2. Three-day averages of (a) east-west flow, (b) relative vorticity, and (c) vertical shear along the Velasco section of Figure 1 during the westward flow study period of December 18, 2016. All panels represent a three-day average from December 17 to December 19 to suppress tidal and inertial contributions to the signal.

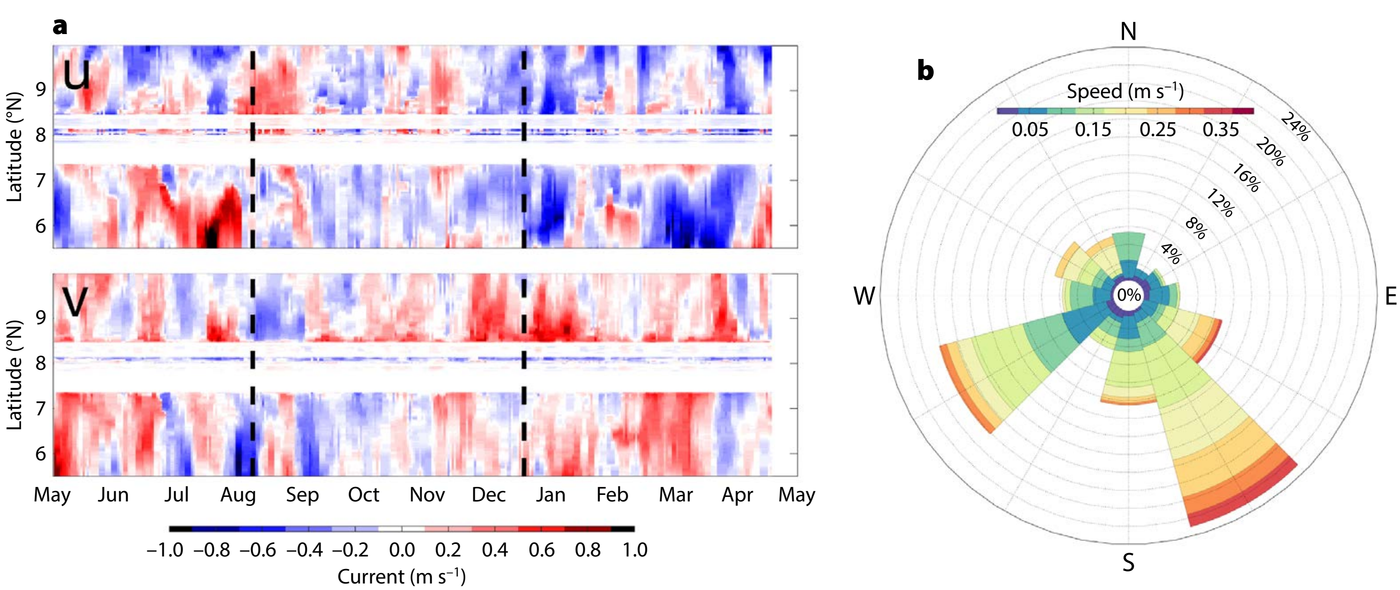

FIGURE 3. (a) East (*u*) and north (*v*) flow vs. time for the Velasco section in Figure 1, averaged over the upper 200 m of the water column. (b) Current rose showing the direction flow is coming from (meteorological convention) and frequency of occurrence. For the current rose plots, currents were averaged over the upper 200 m and from 8°30'N to 9°00'N.

August 2016 study period, the wake from the channels was ultimately swept southward along the eastern side of Palau. An animation of the flow during this month can be found at https://youtu.be/qmu4TlE5Rn8. Further statistics of the flow are discussed in the Flow Statistics section below.

Depth-latitude sections of east-west (u) currents, relative vorticity, and vertical shear (Figure 2a,b,c respectively) reveal that the wake has considerable three-dimensional structure. These signals have been averaged over three days to suppress inertial and tidal contributions. It is worth noting that while the strongest mean currents are at the surface, north of Velasco, relative vorticity is actually strongest in a core at 500 m depth. This strong subsurface vorticity may be associated with the flow crossing the ridge running north from Velasco but occurs almost 1,000 m above bottom (Figure 2b). Also note the complicated layering of the vertical shear in the upper 250 m with amplitudes in excess of 1 m s^{-1} km^{-1} (Figure 2c).

Flow Statistics

During the December 18 westward flow event, the large-scale structure of surface relative vorticity is similar in the high and lower resolutions models (Figure 5a,b). This indicates that the basic flow patterns around Palau are set by the boundary conditions from the REGION model, and in turn are controlled by the large-scale geostrophic flow as represented by, for example, AVISO. However, many of the details differ, not just near Palau but throughout the PALAU domain. It is apparent that the higher resolution allows for sharpening of the fronts, increases the intensity of the vortices, and reduces their spatial scale. Additionally, the frequency of the location and the number of vortices that have been shed from the northern tip of Velasco has changed. In the PALAU model, the eddy shedding period is 34 ± 10 hours as opposed to 50 ± 20 hours in the REGION model. A cross section (dashed line in Figure5a,b) of relative vorticity shows rather different spatial distribution, scales, and intensities (Figure 5c). Power spectral density (PSD) of wavenumber (Figure 5d) is a statistical representation of the distribution of vorticity (i.e., signal "power") as a function of scale (x-axis: wavenumber κ (m^{-1}). The PSD of vorticity in the PALAU model is somewhat weaker at low wavenumbers (long wavelengths), but starting at around 25 km wavelength, the PALAU PSD exceeds that of the REGION model, reflecting a cascade of energy from large to small scales when flow interactions with topography excite small-scale vortices and wakes at the expense of energy in the large-scale current. The spectrum of kinetic energy (not shown) shows that the low-wavenumber kinetic energy of the REGION and PALAU models are similar, but as in vorticity, there is more power at wavelengths below 25 km. This redistribution of spectral power emphasizes the importance of high resolution in simulating the local energy and vorticity balance of the equatorial current systems.

The histogram of vorticity (Figure 6) for the two models differs in several ways. While the mean vorticity in the domain is approximately zero in both the REGION and PALAU models (mu ≈ 0 in Figure 6), the positive skewness (i.e., the asymmetry of the histogram with a bias toward large positive values of vorticity) and kurtosis (a measure of the heavy "tailedness" of the distribution) of both models indicates a shift of the distribution toward negative vorticity, with long tails indi-

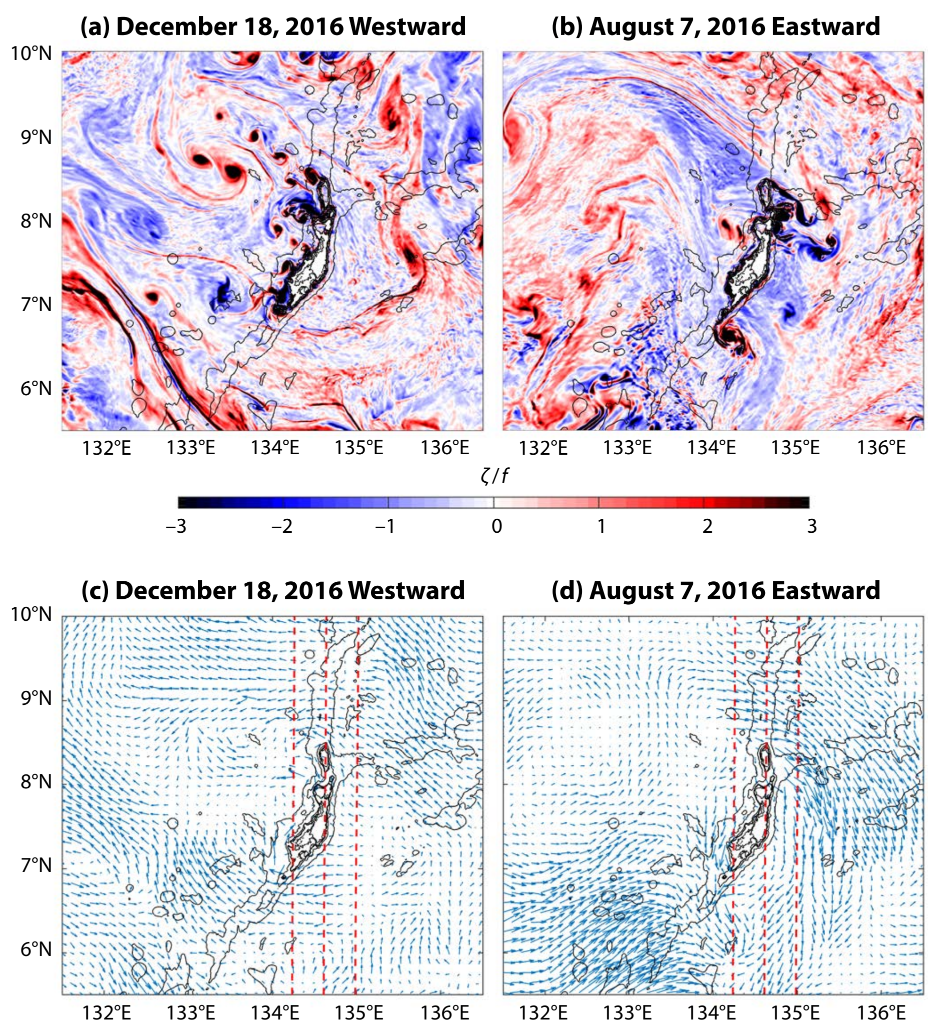

FIGURE 4. Instantaneous surface relative vorticity during (a) westward and (b) eastward flows and currents (c,d) averaged over the upper 200 m.

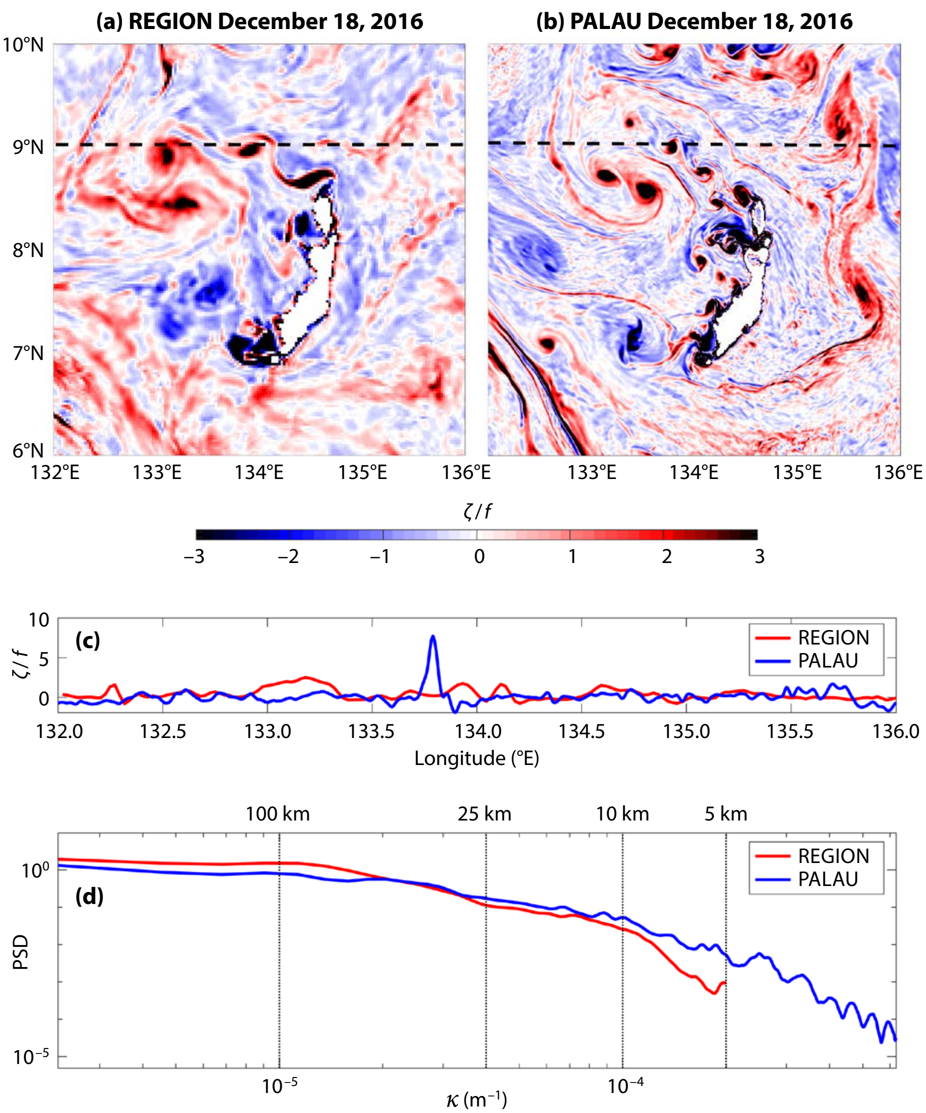

FIGURE 5. Instantaneous (a) REGION and (b) PALAU surface relative vorticity. (c) The instantaneous surface relative vorticity along the section at 9°N indicated in (a) and (b). (d) The wavenumber spectrum of surface relative vorticity is computed here over the full domain shown in (a) and (b).

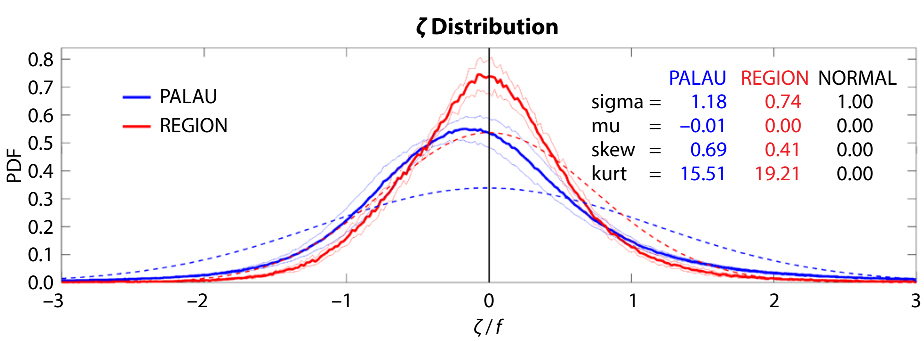

FIGURE 6. Histogram of surface relative vorticity in the PALAU and REGION models during August 2016. Bold lines are the mean histogram, and light lines indicate one standard deviation over the month. Dashed lines indicated a reference normal distribution with mean of zero and standard deviation of one.

cating that there are a number of strong positive vortices of either sign. A small bias toward positive vorticity counterintuitively causes the peak in the histogram to be shifted away from the mean.

DISCUSSION

We have documented the characteristics of the Palau wake from May 2016 through April 2017 using a regional and nested high-resolution model. We one-way nested the PALAU model into the state estimate REGION model, and the PALAU model exhibits the same lower wavenumber characteristics and phase of the vorticity structure as the REGION model (compare Figure 5a,b), but the vorticity at high wavenumbers is shifted significantly to provide improved estimates of the turbulent wakes that develop to both the west and east of Palau (Figure 5c,d). Hence, the low wavenumber structure is largely preserved in the PALAU model, and the gross structures do not diverge, but increased resolution allows higher wavenumbers. The state estimate has improved the REGION representation of the observations, but the PALAU model should be a better prediction of the low-to-high wavenumbers in the flow field, making it ideal for detailed process studies and observational intercomparison.

The increase of vortex shedding frequency at higher resolution is worth noting. The PALAU model exhibits a transition to a different eddy shedding regime as a result of a transition to a higher Reynolds number, as Dong et al. (2007) document. The Strouhal number $St = \omega L/U$ predicts eddy shedding frequency vs. flow rate past an object, where ω is the shedding frequency. Many previous numerical studies (e.g., Perfect et al., 2018) explored steady flow past a submerged obstacle or island. In the case of Palau, the regional flow is extremely variable, making characterization of flow velocity and eddy shedding subjective, so that it is harder to quantify nondenominational characteristics of the flow. Given these caveats, we find that the mean flow across standard sections such as the one north of Velasco change with resolution by only a few percent when averaged over a month. Thus, the change in Reynolds number (Re) and Strouhal number (St) of the flow can be expressed as the ratio of the two model's viscosity and eddy shredding frequencies. Hence, $Re_{PALAU}/Re_{REGION} \approx 6$ and $St_{PALAU}/St_{REGION} \approx 1.5$.

These results show that to capture the characteristics of the wake behind the island of Palau (and other similar obstructions to large mean flows) requires model resolution that is many times higher than the typical first baroclinic mode Rossby radius. Despite the relatively high resolution of the 2.5 km REGION model when compared to global ocean forecast models, it is insufficient to capture the processes of the vortex-street generation at the tips of the geographic features and along the steep slopes of Palau. These features emerge in the 800 m resolution PALAU model and suggest that future process studies of wake generation will require significant computing resources to get to resolutions sufficient for capturing wake energy transfers and cascades.

REFERENCES

Bergh, J., and J. Berntsen. 2008. Numerical studies of wind forced internal waves with a nonhydrostatic model. *Ocean Dynamics* 59:1,025–1,041, https://doi.org/10.1007/s10236-009-0226-1.

Caldeira, R.M.A., P. Marchesiello, N.P. Nezlin, P.M. DiGiacomo, and J.C. McWilliams. 2005. Island wakes in the Southern California bight. *Journal of Geophysical Research* 110(C11), https://doi.org/10.1029/2004JC002675.

Chang, M.-H., T.Y. Tang, C.-R. Ho, and S.-Y. Chao. 2013. Kuroshio-induced wake in the lee of Green Island off Taiwan. *Journal of Geophysical Research* 118(3):1,508–1,519, https://doi.org/10.1002/jgrc.20151.

Courtier, P. 1997. Dual formulation of four-dimensional variational assimilation. *Quarterly Journal of the Royal Meteorological Society* 123:2,449–2,461, https://doi.org/10.1002/qj.49712354414.

Dong, C., J.C. McWilliams, and A.F. Shchepetkin. 2007. Island wakes in deep water. *Journal of Physical Oceanography* 37(4):962–981, https://doi.org/10.1175/JPO3047.1.

Dower, J., H. Freeland, and K. Juniper. 1992. A strong biological response to oceanic flow past Cobb seamount. *Deep Sea Research Part A* 39(7):1,139–1,145, https://doi.org/10.1016/0198-0149(92)90061-W.

Gula, J., M.J. Molemaker, and J.C. McWilliams. 2015a. Topographic vorticity generation, submesoscale instability and vortex street formation in the Gulf Stream. *Geophysical Research Letters* 42(10):4,054–4,062, https://doi.org/10.1002/2015GL063731.

Gula, J., M.J. Molemaker, and J.C. McWilliams. 2015b. Topographic generation of submesoscale centrifugal instability and energy dissipation. *Nature Communications* 7:12811, https://doi.org/10.1038/ncomms12811.

Hamner, W.M., and I.R. Hauri. 1981. Effects of island mass: Water flow and plankton pattern around a reef in the Great Barrier Reef lagoon, Australia. *Limnology and Oceanography* 26(6):1,084–1,102, https://doi.org/10.4319/lo.1981.26.6.1084.

Hernandez-Léon, S. 1991. Accumulation of mesozooplankton in a wake area as a causative mechanism of the "island-mass effect." *Marine Biology* 109:141–147, https://doi.org/10.1007/BF01320241.

Heywood, K.J., D.P. Stevens, and G.R. Bigg. 1996. Eddy formation behind the tropical island of Aldabra. *Deep Sea Research Part I* 43(4):555–578, https://doi.org/10.1016/0967-0637(96)00097-0.

Janeković, I., and B.S. Powell. 2012. Analysis of imposing tidal dynamics to nested numerical models. *Continental Shelf Research* 34:30–40, https://doi.org/10.1016/j.csr.2011.11.017.

Large, W.G., J.C. McWilliams, and S.C. Doney. 1994. Oceanic vertical mixing: A review and a model with non-local boundary layer parameterization. *Review of Geophysics* 32:363–403, https://doi.org/10.1029/94RG01872.

Mason, E., J. Molemaker, A.F. Shchepetkin, F. Colas, J.C. McWilliams, and P. Sangra. 2010. Procedures for offline grid nesting in regional ocean models. *Ocean Modelling* 35(1):1–15, https://doi.org/10.1016/j.ocemod.2010.05.007.

May, D., M. Parmeter, D. Olszewski, and B. McKenzie. 1998. Operational processing of satellite sea surface temperature retrievals at the Naval Oceanographic Office. *Bulletin of the American Meteorological Society* 79(3):397–407, https://doi.org/10.1175/1520-0477(1998)079<0397:OPOSSS>2.0.CO;2.

Merrifield, S.T., P.L. Colin, T. Cook, C. Garcia-Moreno, J.A. MacKinnon, M. Otero, T.A. Schramek, M. Siegelman, H.L. Simmons, and E.J. Terrill. 2019. Island wakes observed from high-frequency current mapping radar. *Oceanography* 32(4):92–101, https://doi.org/10.5670/oceanog.2019.415.

Molemaker, M.J., J.C. McWilliams, and W.K. Dewar. 2015. Submesoscale instability and generation of mesoscale anticyclones near a separation of the California Undercurrent. *Journal of Physical Oceanography* 45(3):613–629, https://doi.org/10.1175/JPO-D-13-0225.1.

Perfect, B., N. Kumar, and J.J. Riley. 2018. Vortex structures in the wake of an idealized seamount in rotating, stratified flow. *Geophysical Research Letters* 45(17):9,098–9,105, https://doi.org/10.1029/2018GL078703.

Shchepetkin, A.F., and J.C. McWilliams. 2005. The Regional Oceanic Modeling System (ROMS): A split-explicit, free-surface, topography-following-coordinate ocean model. *Ocean Modelling* 9:347–404, https://doi.org/10.1016/j.ocemod.2004.08.002.

Smith, W.H.F., and D.T. Sandwell. 1997. Global sea floor topography from satellite altimetry and ship depth soundings. *Science* 277:1,956–1,962, https://doi.org/10.1126/science.277.5334.1956.

Zedler, S.E., B.S. Powell, B. Qiu, and D.L. Rudnick. 2019. Energy transfer in the western tropical Pacific. *Oceanography* 32(4):136–145, https://doi.org/10.5670/oceanog.2019.419.

ACKNOWLEDGMENTS

This work was supported by the Office of Naval Research. HLS was supported by grant numbers N00014-17-1-2383 and N00014-13-1-0452. BSP and SZ were supported by grant number N00014-15-1-2600. The Palau National Government provided permits for all relevant shipboard and land-based work.

AUTHORS

Harper L. Simmons (hlsimmons@alaska.edu) is Associate Professor, College of Fisheries and Ocean Sciences, University of Alaska Fairbanks, Fairbanks, AK, USA. **Brian S. Powell** is Professor, Department of Oceanography, University of Hawaiʻi at Mānoa, Honolulu, HI, USA. **Sophia T. Merrifield** is Project Scientist, Scripps Institution of Oceanography, University of California San Diego, La Jolla, CA, USA. **Sarah E. Zedler** is a researcher at the National Oceanography Centre, Liverpool, UK. **Patrick L. Colin** is Director, Coral Reef Research Foundation, Koror, Palau.

ARTICLE CITATION

Simmons, H.L., B.S. Powell, S.T. Merrifield, S.E. Zedler, and P.L. Colin. 2019. Dynamical downscaling of equatorial flow response to Palau. *Oceanography* 32(4):84–91, https://doi.org/10.5670/oceanog.2019.414.

COPYRIGHT & USAGE